Compositional variation and genesis of ferromanganese crusts of the Afanasiy–Nikitin Seamount, Equatorial Indian Ocean

R P Rajani, V K Banakar*, G Parthiban, A V Mudholkar and A R Chodankar

National Institute of Oceanography, Dona Paula, Goa 403 004, India.
** e-mail: banakar@darya.nio.org*

Eight ferromanganese crusts (Fe–Mn crusts) with igneous and sedimentary substrates collected at different water depths from the Afanasiy–Nikitin Seamount are studied for their bulk major, minor and rare earth element composition. The Mn/Fe ratios < 1.5 indicate the hydrogenetic accretion of the Fe–Mn hydroxides. These Fe–Mn crusts are enriched in Co (up to 0.9%, average $\sim 0.5\%$) and Ce. The Ce-content is the highest reported so far (up to 3763 ppm, average ~ 2250 ppm) for global ocean seamount Fe–Mn crusts. In spite of general similarity in the range of major, minor, and strictly trivalent rare earth element composition, the dissimilarity between the present Fe–Mn crusts and the Pacific seamount Fe–Mn crusts in Co and Ce associations with major mineral phases indicates inter-oceanic heterogeneity and region-specific conditions responsible for their enrichment. The decrease in Ce-anomaly (from ~ 8 to ~ 1.5) with increasing water depth (from ~ 1.7 km to ~ 3.2 km) might suggest that the modern intermediate depth low oxygen layer was shifted and sustained at a deeper depth for a long period in the past.

1. Introduction

The Afanasiy–Nikitin Seamount (ANS) located at 3°S latitude and 83°E longitude in the Equatorial East Indian Ocean (EEIO) (figure 1) was discovered during the R. V. Vityaz cruise of 1959 (Bogorov and Bezrukov 1961). It was shown to have formed during the Late-Cretaceous (Mahoney *et al* 1996; Levechenko 1990; Sborshchikov *et al* 1995). The ANS has evolved as a part of an 85°E ridge (Borisova *et al* 2001). Although the Russian researchers extensively explored the ANS with the help of the 'Mir' submersible, we are not aware of any published literature on the occurrence of Co-enriched Fe–Mn crusts. The first report of the Co-enriched Fe–Mn crusts from the ANS was that of Banakar *et al* (1997) based on the results of R. V. A. A. Sidorenko cruise of 1994. They also demonstrated, based on the characteristics of the substrate rocks, that the ANS was exposed to sub-aerial conditions after its emplacement. Subsequent to its emplacement the ANS has undergone tectonic disturbances due to intraplate deformation episodes in the region (Srikrishna *et al* 2001) as evidenced by numerous criss-cross faults of the seamount (Rudenko 1994). The ANS gains significance not only because of its tectonic history but also due to the presence of potentially economically important Co-enriched Fe–Mn crusts (Parthiban and Banakar 1999).

Fe–Mn crusts cap most of the seamounts in the world oceans, where the shallow-water seamount Fe–Mn crusts are generally enriched in Co compared to their deep-sea counterparts (Hein *et al* 1988; Hein *et al* 2000). The seamount Fe–Mn crusts deposited in the hydrothermally inactive regions are exclusively of hydrogenetic origin because of the non-availability of diagenetically remobilised metals due to the absence of sediment cover. Most of the free and complexed transition and alkali-

Keywords. Ferromanganese crusts; composition; seamount; Equatorial Indian Ocean.

J. Earth Syst. Sci., **114**, No. 1, February 2005, pp. 51–61

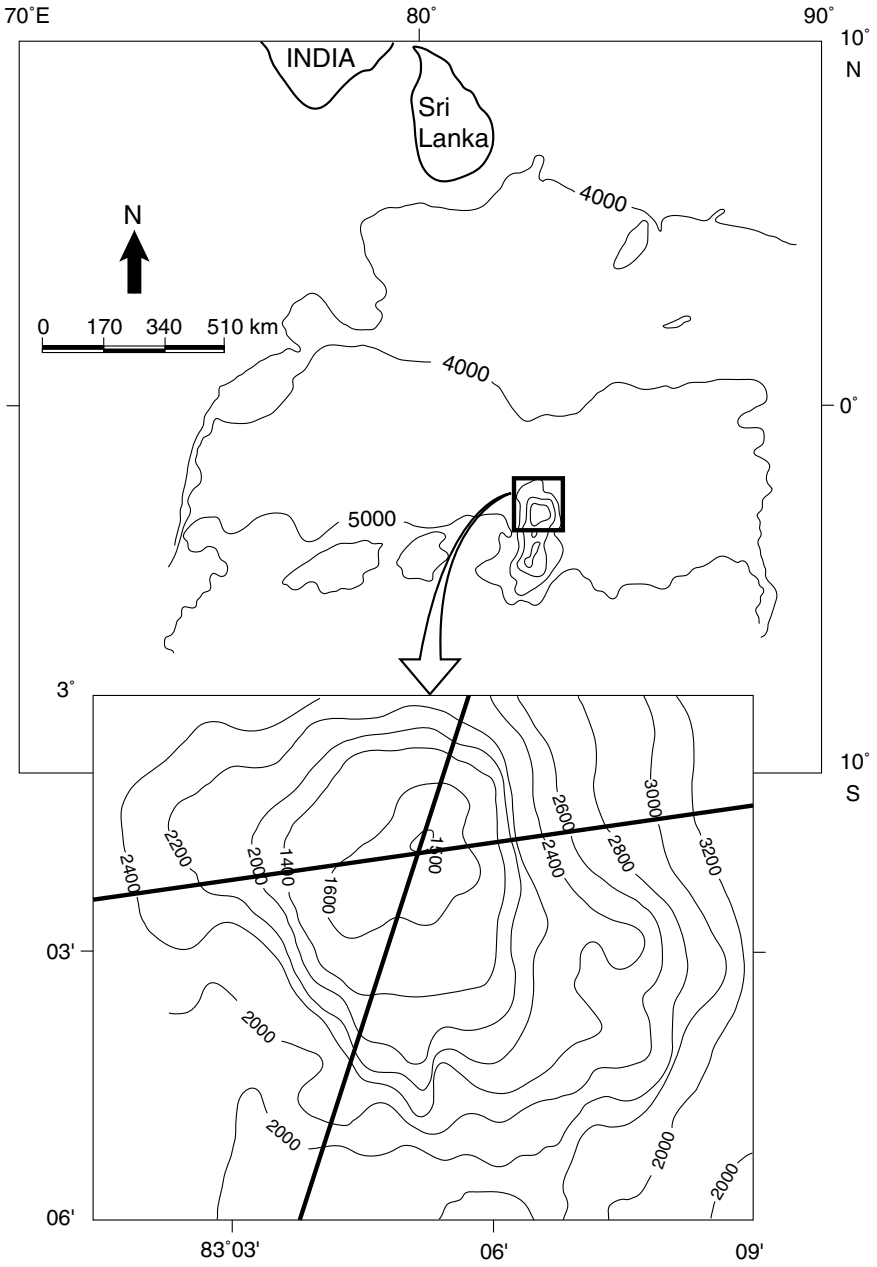

Figure 1. Location of the Afanasiy–Nikitin Seamount in the Equatorial Indian Ocean. The open square indicates the sampled area, which is shown as exploded inset. The thick lines are the sampling transects during two cruises; CC1 is AA Sidorenko Cobalt Crust Cruise 1 and CC2 is AA Sidorenko Cobalt Crust Cruise 2. The contours are the water depths.

metals are preferentially removed from the ambient water by adsorption on to the negatively charged surfaces of MnO_2 colloids, while negatively charged ions become preferentially bound to the slightly positively charged FeOOH phase during Fe–Mn crust formation (Koschinsky and Hein 2003). Hydrogenous Fe–Mn crusts accumulate by slow accretion (< 10 mm/Ma) of Fe–Mn oxyhydroxides precipitated from ambient seawater (Halbach *et al* 1983; Segl *et al* 1984, Hein *et al* 1988; Manheim and Lane-Botswick 1988; Banakar and Borole 1991; Frank *et al* 1999). The slow growth rate allows for effective adsorption of a considerable quantity of minor elements by the oxyhydroxide colloids during the process of Fe–Mn crust accretion (Koschinsky and Halbach 1995). Most likely, the Fe-hydroxide precipitate forms the primary layer during the hydrogenetic accretion of the crust oxide, which subsequently catalyses the oxidation of Mn (Burns and Brown 1972). The further growth process of the Fe–Mn crusts is believed to be autocatalytic. However, it is difficult to show this initial fractionation of Fe and Mn from the ambient water because they are intimately intermixed. The dominant controls on the incorporation of various metals in the Fe–Mn crusts

include their concentrations in seawater, surface-charge and -area of colloidal particles, and growth rate (Halbach *et al* 1983; 1989). Utilizing characteristic fractionation of different metals, several previous workers have demonstrated the potential of seamount Fe–Mn crusts as a repository of past-oceanic conditions (see Banakar and Hein 2000 and references therein). One such group of metals for example is the lanthanides (Rare Earth Elements: REE) and Co. The REE were shown to fractionate during the Fe–Mn crust formation (Elderfield 1988; De Carlo 1991; De Carlo and McMurtry 1992; Bau *et al* 1996; Banakar *et al* 1997). The Co and Ce were shown to readily oxidize to their higher oxidation state on adsorption to negatively charged Mn and slightly positively charged Fe–Ti colloidal particles respectively. Therefore, the Co- and Ce-enrichment provide a useful tool to understand the oxygenation conditions of the ambient water in which the Fe–Mn crusts have formed. However, these relationships may not be valid in the presence of phosphatic intergrowth in the Fe–Mn crusts or when the role of kinetic fractionation is dominant during the growth of Fe–Mn crusts (Bau *et al* 1996).

The Fe–Mn crusts exhibit enrichment of metals compared with their ambient seawater concentration by many orders of magnitude (Koschinsky and Halbach 1995), and most dominantly enriched metal species are those of the transition group comprising Mn, Fe, Co, Ni, Cu, V, Pb, Zn, etc. The group of elements that is second most enriched is the REEs, followed by ultra-trace metals such as platinum group elements. Although considerable work has been carried out on Fe–Mn crusts of the world oceans, not many studies on Indian Ocean Fe–Mn crusts were carried out (Iyer 1991; Frank and O'Nions 1998; Frank *et al* 1999; Banakar and Hein 2000 and references therein). Particularly, studies on ANS Fe–Mn crust are extremely sparse and were based on samples collected from a single dredging-operation from the upper flank of the ANS (Banakar *et al* 1997; Parthiban and Banakar 1999). In this paper we present bulk chemical data of Fe–Mn crusts collected from different water depths from the ANS and address the genetic aspects of those deposits utilizing the compositional variations. We are aware that the bulk chemistry of Fe–Mn crusts does not provide past changes in the accretionary environment. However, it helps in understanding the dominant processes responsible for their formation.

2. Material and methods

The Fe–Mn crust samples from the ANS in the EEIO (figure 1) were collected during two cruises of R. V. A. A. Sidorenko as part of the ongoing 'Cobalt-Crust' project supported by the Department of Ocean Development and the National Institute of Oceanography. The thickness of the Fe–Mn crust layer on the substrate rocks varies from coating to ~ 7 cm. For the present study we have selected only eight samples having at least ~ 1 cm thick Fe–Mn oxide layer to avoid dilution of the crust-oxide by substrate-rock material. The samples included are from a total depth range of 1700–3200 m and are free from any visible change in the colour within the vertical section of the oxide layer. Normally the presence of phosphatic layers (light coloured) alter chemical characters of the hydrogenetically precipitated oxide material (Bau *et al* 1996; Banakar *et al* 1997), it is necessary therefore to avoid such samples for genetic interpretations following the bulk chemical composition. The top of the seamount is located at a depth of 1650 m (Rudenko 1994). The two main types of substrate rocks found on the ANS are basalts (fresh and altered) and a variety of limestone. The thicker Fe–Mn oxide layer generally occurs on basaltic substrates, while thin (few micron to few mm) Fe–Mn oxide layers were deposited on the limestone substrates. At deep-water locations (> 2500 m) the Fe–Mn oxide layer thickness ranges from 2 to 4 cm and was accreted on the columnar basalts. Large boulders of conglomerates, beach-rocks, and fossil corals coated with Fe–Mn oxide were also recovered. The details of the petrography and petrochemistry of the substrate rocks will be reported elsewhere. The Fe–Mn crust layers were chipped off from the substrate and analysed for ten major and minor elements (Mn, Fe, Ti, Cu, Co, Ni, Zn, Pb, V, and Mo) on an Optima-2000 DV ICP-AES using the 6N HCl leachates obtained by extracting the oxide fraction from the finely powdered and overnight oven dried (~ 105°C) sample aliquots. The mixture was repeatedly heated to ensure complete extraction of the oxides as evident by white silicate residue retained on the filter paper. This procedure however, may not prevent certain dissolution of clay fraction if present along with the Fe–Mn oxides. The REE measurements were carried out at the ICP-MS facility of NGRI, Hyderabad, India. The USGS-A1 and -P1 standards were used for estimating analytical accuracy, which was better than $\pm 3\%$ in case of major and minor metals and $\pm 5\%$ in case of REE.

The inter-element associations were determined using CORREL software available in Microsoft-Excel applications, and only the significant associations ($R => 0.6$ at 99% confidence level for $n = 8$) are discussed. The Ce-anomaly (Ce/Ce^*) was calculated from the shale (NASC: Haskin and Haskin 1966; Piper 1974) normalized (SN) REE content of the samples as $Ce/Ce^* = 2Ce_{SN}/La_{SN} + Pr_{SN}$ (Murray *et al* 1991). The growth rate of the crusts

Table 1. *Major and minor element composition of Fe–Mn crusts from the Afanasiy–Nikitin Seamount.*

	Depth	Mn	Fe	Ti	Cu	Ni	Co	Zn	Pb	V	Mo	Mn/Fe	GR[1]	GR[2]
CC1/DR/10C	1.7	15.9	17.0	0.94	0.07	0.19	0.57	514	1516	481	218	0.9	1.73	1.12
CC1/DR/25	1.8	15.5	16.0	0.70	0.08	0.19	0.48	539	1324	436	250	1.0	2.35	1.84
CC1/DR/12B	1.9	18.0	14.2	0.66	0.08	0.23	0.48	431	1423	430	338	1.3	2.33	1.81
CC2/ADR/27	2.1	24.9	24.2	1.15	0.07	0.37	0.86	724	2305	709	438	1.0	0.88	0.38
CC2/ADR/11	2.2	18.7	19.5	0.75	0.05	0.24	0.50	588	1727	550	340	1.0	2.19	1.65
CC2/ADR/12	2.5	21.3	14.0	0.93	0.06	0.31	0.47	1318	1891	656	518	1.5	2.33	1.86
CC2/ADR/18	2.6	18.1	24.3	1.48	0.17	0.23	0.42	1553	2347	710	290	0.7	2.94	2.64
CC2/ADR/24A	3.2	22.2	22.6	0.75	0.11	0.25	0.30	734	1802	738	494	1.0	5.07	6.36
Atlantic*		12.7	22.9	1.00	0.08	0.30	0.35	587	1133	855	435	0.6		
Indian*		13.5	20.2	0.90	0.15	0.30	0.33	512	1027	573	334	0.7		
NW-Pacific*		22.1	15.1	0.77	0.10	0.54	0.64	680	1777	515	455	1.5		

Depth in km; Mn through Co in wt%; Zn through Mo in ppm; GR = growth rate in mm/Ma based on Cobalt-model of 1 – Manheim and Lane-Bostwick (1988), and 2 – Frank *et al* (1999).
*Data from Hein *et al* (2000).

was determined using the Co-based age models derived by Manheim and Lane-Bostwick (1988) [growth rate (mm/Ma) = $0.68/\mathrm{Co_w^{1.67}}$, where $\mathrm{Co_w}$ is the detrital background (0.0012 wt.%) corrected Co content]; and ^{10}Be-tuned Co-model of Frank *et al* (1999) [growth rate (mm/Ma) = $0.25/\mathrm{Co^{2.69}}$]. Even though both these models yield comparable growth rates (table 1), the uncertainty is large with such empirical relationships. Therefore, the maximum ages assigned to the specimen are approximate ages.

3. Results and discussion

3.1 *The substrate rocks*

The substrates for the Fe–Mn crust accretion in the ANS region comprise mainly basalts and a variety of sedimentary rocks including fossil corals. Most of the basalts are massive, compact, and have vesicles with varying volume percentages. The vesicles are of various shapes but in general, small sized. Few basalts exhibit, circular vesicles, which are filled with sediment. These basalts are dull yellow in colour, compact, and without vesicles. The columnar jointing might have formed due to slow cooling and simultaneous contraction of the basaltic lava when developing the joint planes. The basalts of the ANS belong to the Late-Cretaceous basaltic effusions at the time of emplacement of the seamount (Levechenko 1990). They are mostly grey to black and porphyritic. In general, the basalts are plagioclase-phyric with plagioclase mega-crysts (8–10 mm) and phenocrysts (4–5 mm) embedded in the glassy ground mass. Within the groundmass small phenocrysts of ortho- and clino-pyroxene and smaller olivine crystals are observed. Few types of basalts are aphanatic with micro-phenocrysts of plagioclase showing flow texture. The major element composition of the basalts was processed for the CIPW norm calculation based on the SINCLAS program (Verma *et al* 2002), which suggests that basalts are trachy-andesites, potassic trachy-basalts and basanites. These rocks are rich in alkalies with average total alkali content of $\sim 7\%$ and with high phosphate content varying from $\sim 1\%$ to 4.5%.

Sedimentary rocks from the ANS are mostly carbonate-rich. They occur along the upper flanks of the seamount. The rounded basalt-clasts and large brachiopod shells embedded in the calcareous cement support the earlier view of sub-aerial exposure of the ANS to high-energy environments (Banakar *et al* 1997). The fossilized coralline substrates coated with the Fe–Mn oxide provide unambiguous further support for the significantly shallower water depth over the ANS in the past. The Fe–Mn crust substrates from 2000–2500 m water depths are generally brecciated, which may be a consequence of extensive post-emplacement faulting in the region.

3.2 *Compositional variation*

The major and minor element composition and growth rates of the ANS Fe–Mn crusts are presented in table 1 and the REE composition in table 2. The Mn/Fe ratios vary from 0.7 to 1.5 indicating that the formation of Fe–Mn crusts in this region was dominantly by hydrogenetic precipitation of Mn and Fe hydroxides (Bonatti *et al* 1972; Halbach *et al* 1983). The Co-enrichment in seamount Fe–Mn crusts is well known and has been documented from many seamounts of the Pacific, where its content reaches up to 2% (Halbach and

Table 2. *Rare earth element composition of the Afanasiy–Nikitin Seamount Fe–Mn crusts.*

	La	Ce	Pr	Sm	Eu	Gd	Dy	Ho	Er	Yb	Lu	Ce*
CC1/DR/10C	291	3763	41.0	34.7	8.2	57.4	36.5	9.5	19.1	22.8	3.5	8.1
CC1/DR/25	287	2860	44.7	39.3	9.1	51.8	40.1	10.2	20.3	24.3	3.8	6.0
CC2/ADR/12	597	2028	39.5	33.0	8.0	51.3	40.1	11.1	22.6	26.7	4.4	2.7
CC1/DR/12B	287	2561	47.8	43.6	10.0	53.9	44.1	11.1	21.3	25.6	3.8	5.3
CC2/ADR/27	584	1884	45.0	39.6	9.4	54.4	41.5	10.4	20.1	13.3	1.7	2.4
CC2/ADR/11	242	1328	41.6	38.3	9.1	46.4	39.1	9.7	18.5	21.8	3.5	3.2
CC2/ADR/18	211	2206	33.2	29.0	6.9	44.1	28.0	6.8	13.0	15.4	2.5	6.3
CC2/ADR/24A	625	1349	52.2	49.3	12.1	62.7	55.4	13.9	26.7	31.7	5.0	1.6
Average-ANS	390	2247	43.1	38.4	9.1	53	40.6	10.3	20.2	22.7	3.7	
NW-Pacific*	202	1105	106	41.6	9.9	26	57.8	6.6	31.9	17.7	3.3	
Hawali**	287	1277	53.7	50.5	14.0	61	48.7		26.5	25.3	3.6	
Kiribati†	155	606	24.1	19.0	5.0	28.1	25.2		18.7	18.1		
Line-Island‡	307	1100	56.0	54.0	14.0	55	52.0		31.0	28	4.2	

*Hein *et al* (2000), **De Carlo *et al* (1992), †Wen *et al* (1997), ‡Aplin (1984).

Puteanus 1984; Hein *et al* 1988). At the outset, based on previous observations, the Co-enrichment can be explained by the ability of positively charged Co^{2+} to adsorb to the negatively charged MnO_2-colloidal surfaces and subsequent oxidation to Co^{3+} due to the surface enrichment and strong electric field at the colloid-solution interface (Halbach *et al* 1983; De Carlo and McMurtry 1992; Wen *et al* 1997). The depletion of Ni and Cu in the ANS Fe–Mn crusts compared with abyssal Fe–Mn nodules can be explained by the absence of diagenetically remobilised pool of transition metals due to sediment-free substrates on the seamounts. In general the composition of the present Fe–Mn crusts resembles the composition of world ocean seamount Fe–Mn crust deposits (table 1 and also see De Carlo and McMurtry 1992; Wen *et al* 1997; Frank *et al* 1999; Hein *et al* 2000). This broad compositional similarity of the Fe–Mn crusts occurring on seamounts of different oceans suggests nearly similar genetic aspects as well as the metal up-take mechanism. On the other hand, the REE composition of the ANS Fe–Mn crusts exhibits distinct disagreement with the Pacific Fe–Mn crusts in both their relationship with major mineral phases and Ce-content (tables 2 and 3). The trivalent-REE (T-REE) content of the ANS and Pacific Fe–Mn crusts are more or less in the same range, but the Ce is significantly enriched in the ANS Fe–Mn crusts. The Ce/Ce^* is highly positive (figure 2) and reaches up to 8 in the specimen from the upper most flank of the ANS (table 2, figures 2 and 3). Considering the Ce-content and Ce/Ce^* as indicators of redox conditions (Elderfield 1988; De Carlo 1991; De Carlo and McMurtry 1992; Bau *et al* 1996; Banakar *et al* 1997), the ANS Fe–Mn crusts appear to have accreted in better oxygenated waters compared with the ambient waters of the Pacific Fe–Mn crusts. Presently a low oxygen layer (with dissolved O_2 over 1.5 ml/L) between 500 m and 1500 m water depth characterizes the EEIO region (Wyrtki 1971: figure 3). The EEIO in which the ANS is located might have not experienced therefore OMZ conditions (dissolved $O_2 < 0.5$ ml/L) in the past several millions of years represented by the Fe–Mn crusts. This better-oxygenated intermediate depth water in the ANS-region should explain the significant enrichment of Ce in the present Fe–Mn crusts. The T-REE content of the ANS, Hawaii, and Line-Island Fe–Mn crusts (Aplin 1984; De Carlo *et al* 1992) is nearly in the same range but distinctly higher than the Kiribati Fe–Mn crusts (Wen *et al* 1997) (table 2) suggesting the importance of local hydrochemistry in controlling the REE content of the Fe–Mn crusts, which is clearly evident in the inter-element associations.

3.3 *Inter-element associations*

The inter-element relationships in the Fe–Mn crusts provide useful information on the associations of various minor elements with the major mineral phases, as well as their fractionation from the dissolved pool. Based on the correlation matrix (table 3), it is possible to divide the elements into two main groups defined by mutually strong sympathetic behaviour. Ni, Mo, V, Pb, and La exhibit strong sympathetic association with Mn ($R > 0.7$) forming the MnO_2 phase, while Fe and Ti are mutually coherent ($R = 0.6$) indicating the presence of Fe–Ti hydrate phase. As the Ti is a hydroxide dominated element it tends to form mixed oxide phase with Fe (Koschinsky and Halbach 1995; Bau *et al* 1996). The minor metals such as Pb and V

Table 3. *Inter-element correlations of the Afanasiy–Nikitin Seamount Fe–Mn crust composition.*

	Depth	Mn	Fe	Ti	Cu	Ni	Co	Zn	Pb	V	Mo	Mn/Fe	GR	La	Ce	Pr	Sm	Eu	Gd	Dy	Ho	Er	Yb	Lu	Ce*
Depth	1.0																								
Mn	0.5	1.0																							
Fe	0.5	0.5	1.0																						
Ti	0.2	0.2	**0.6**	1.0																					
Cu	0.5	−0.1	**0.6**	**0.6**	1.0																				
Ni	0.2	**0.9**	0.3	0.3	−0.2	1.0																			
Co	−0.5	0.4	0.2	0.3	−0.5	**0.6**	1.0																		
Zn	0.5	0.2	0.3	**0.8**	**0.6**	0.3	−0.2	1.0																	
Pb	0.5	**0.7**	**0.8**	**0.9**	0.4	**0.7**	0.3	**0.7**	1.0																
V	**0.8**	**0.8**	**0.7**	**0.6**	0.4	**0.6**	0.0	**0.7**	**0.9**	1.0															
Mo	**0.7**	**0.9**	0.1	−0.1	−0.1	**0.8**	0.0	0.3	0.4	**0.7**	1.0														
Mn/Fe	0.0	**0.3**	**−0.7**	**−0.4**	**−0.6**	0.4	0.0	0.0	−0.2	−0.1	**0.6**	1.0													
GR	**0.8**	0.2	0.3	−0.2	0.5	−0.2	**−0.8**	0.1	0.0	0.4	0.4	−0.2	1.0												
La	0.5	**0.8**	0.1	−0.1	−0.2	**0.7**	0.2	0.1	0.3	**0.6**	**0.9**	0.5	0.3	1.0											
Ce	**−0.7**	**−0.7**	−0.5	0.0	−0.1	−0.5	0.2	−0.2	−0.5	**−0.6**	**−0.7**	−0.1	−0.4	−0.4	1.0										
Pr	0.2	0.3	−0.1	**−0.7**	−0.3	0.1	−0.1	**−0.7**	−0.4	−0.1	0.3	0.2	0.4	0.5	−0.2	1.0									
Sm	0.3	0.3	0.0	**−0.7**	−0.2	0.0	−0.2	**−0.6**	−0.4	−0.1	0.3	0.1	0.5	0.4	−0.3	**1.0**	1.0								
Eu	0.4	0.4	0.1	**−0.6**	−0.1	0.1	−0.2	**−0.6**	−0.3	0.1	0.4	0.1	**0.6**	0.5	−0.4	**1.0**	**1.0**	1.0							
Gd	0.2	0.3	−0.1	−0.5	−0.2	0.1	0.0	−0.5	−0.3	0.0	0.3	0.2	0.4	**0.6**	0.1	**0.8**	**0.7**	**0.7**	1.0						
Dy	0.4	0.4	−0.1	**−0.7**	−0.2	0.2	−0.2	−0.5	−0.3	0.1	**0.6**	0.3	**0.6**	**0.6**	−0.4	**0.9**	**0.9**	**1.0**	**0.8**	1.0					
Ho	0.4	0.4	−0.2	**−0.7**	−0.3	0.2	−0.2	−0.4	−0.3	0.1	**0.6**	0.5	**0.6**	**0.7**	−0.3	**0.9**	**0.9**	**0.9**	**0.8**	**1.0**	1.0				
Er	0.3	0.4	−0.3	**−0.7**	−0.4	0.2	−0.2	−0.4	−0.4	0.1	**0.6**	0.5	0.5	**0.7**	−0.3	**0.8**	**0.8**	**0.8**	**0.8**	**0.9**	**1.0**	1.0			
Yb	0.3	−0.1	−0.5	**−0.7**	−0.2	−0.3	**−0.7**	−0.3	**−0.6**	−0.2	0.3	0.4	**0.6**	0.3	−0.1	**0.6**	**0.6**	**0.6**	**0.6**	**0.7**	**0.8**	**0.8**	1.0		
Lu	0.4	−0.2	−0.5	**−0.7**	−0.1	−0.4	**−0.8**	−0.1	**−0.6**	−0.2	0.3	0.4	0.7	0.2	−0.1	0.5	0.5	0.5	0.4	**0.6**	**0.7**	**0.7**	**1.0**	1.0	
Ce*	**−0.6**	**−0.8**	−0.3	0.2	0.2	**−0.7**	0.0	−0.1	−0.4	**−0.6**	**−0.9**	−0.4	−0.4	**−0.8**	**0.9**	−0.4	−0.5	**−0.6**	**−0.2**	**−0.6**	**−0.6**	**−0.6**	−0.2	−0.2	1.0

R values > 0.6 (bold) are significant at 99% confidence level; GR = growth rate; Ce* = cerium anomally.

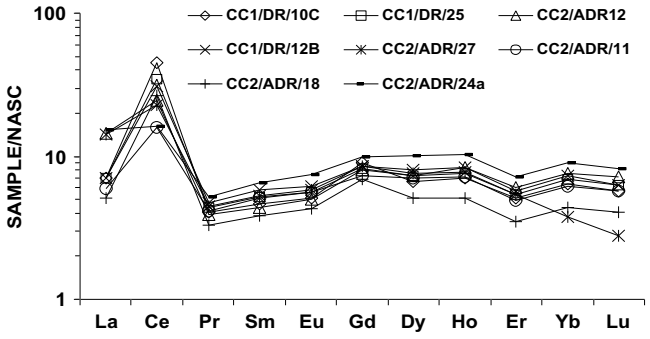

Figure 2. Shale-normalised rare earth element patterns of the Afanasiy–Nikitin Seamount ferromanganese crusts.

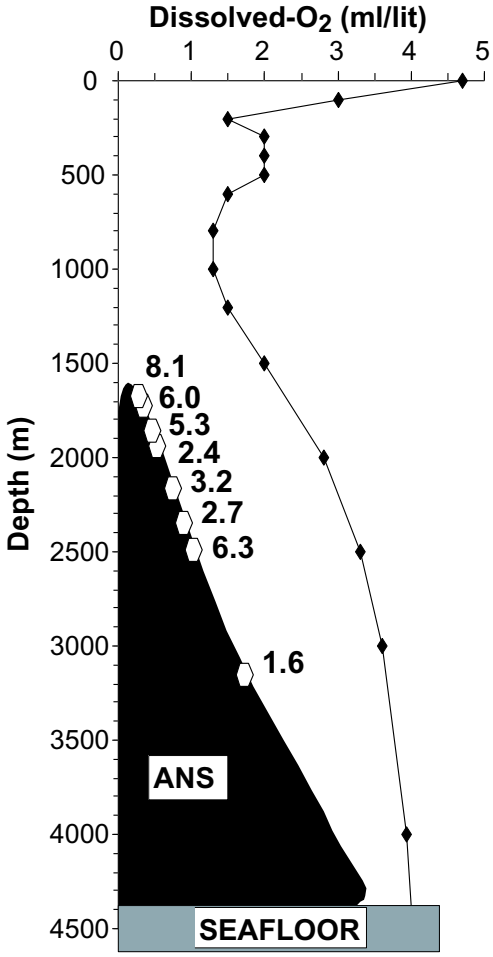

Figure 3. Depth variation of the Ce-anomaly (indicated by values) adjacent to respective Fe–Mn crust locations (open hexagon), and the modern dissolved oxygen depth-profile in the Afanasiy–Nikitin Seamount (ANS: shaded topographic feature) region. Note the gradually decreasing Ce-anomaly with water depth.

are also strongly associated with Fe–Ti phase ($R > +0.6$), suggesting their bimodal association.

Interestingly, the redox-sensitive Co and Ce exhibit inverse association ($R > 0.5$) with water depth in the ANS region (table 3, figure 4). But Co does not associate significantly with any of the above two major mineral phases, and the Ce exhibits strong inverse relationship with Mn ($R = 0.7$). This observation is in contrast with the results of Pacific Fe–Mn crusts (De Carlo 1991), which have demonstrated Mn, Co, Ni and Cu as one co-precipitated group and Fe, Ti, Pb, and Ce as another co-precipitated group. At the outset this independent behaviour of Co and Ce in the ANS Fe–Mn crusts may suggest their precipitation as Co- and Ce-oxides similar to other two major mineral phases instead depending upon the availability of Mn or Fe hydroxide colloids. If they are precipitated as a separate oxide phase then both the elements are expected to exhibit mutually coherent behaviour, which is not evident in the correlation matrix ($R = 0.2$, table 3). This low coherence is the result of two outliers (enclosed by boxes in figure 4). When these outliers are ignored the coherence between Co and Ce increases remarkably ($R = 0.9$, figure 4). Thus the Co and Ce together in fact appear to have incorporated as a separate oxide phase in the ANS Fe–Mn crusts. This is possible because of better-oxygenated intermediate waters bathing the ANS, which might be the reason for the very high concentration of Ce (up to 3760 ppm and average $\sim$ 2250 ppm: table 2). Nevertheless, the other processes such as biological activity influencing the Ce-enrichment or Ce/Ce^* (Wen and De Carlo 1994) cannot be ruled-out. Recent measurements of primary productivity in the ANS-region indicated oligotrophic conditions throughout the year (N Ramaih 2004, personal communication). Further, Co and Ce do not exhibit significant sympathetic association with presently available biologically associated minor elements such as Cu and Zn (table 3). Thus the possibility of biologically mediated Ce-enrichment or Ce/Ce^* development in the ANS Fe–Mn crusts is rather weak. The Co association with Mn, Fe, and Ti is weak ($R < +0.4$), and Ce association with Mn and Fe is negative ($R > -0.5$) (table 3). Such inter-elemental relationships clearly rule-out the possibility of oxidative scavenging by Mn or Fe–Ti hydroxides. Therefore, the high Co and significant enrichment of Ce in the ANS Fe–Mn crusts has been most likely the result of their incorporation as an independent oxide phase.

Various elemental associations in the ANS Fe–Mn crusts do not exhibit strict similarity with those observed in the Pacific seamount Fe–Mn crusts probably because of significant differences in oxygenation of the waters bathing seamounts of the Pacific and the EEIO. The redox sensitive Mn and Co behaviour with increasing depth shows distinct deviations from general trends at $\sim$ 2000 m depth (figure 5). They exhibit maximum concentration at

around this depth while the decreasing Ce-anomaly changes to nearly uniform values below that depth except for the sample located at 2570 m depth (figures 3 and 5). Excluding this depth-specific deviation, the increasing Mn-content with depth associated with decreasing Co- and Ce-content and Ce-anomaly characterises the variations in the first order redox-sensitive metals. Such depth-dependent behaviour of the redox-sensitive metals warrants attention. Contrasting behaviour of Mn and Co with depth has already been observed in the Central Pacific seamount Fe–Mn crusts (Halbach *et al* 1983), in which Co is associated inversely with growth rate, while Mn exhibits sympathetic association. The co-variation of Ce with Co and inverse-variation of Ce/Ce^* with Mn (see figures 4 and 5) suggest a common mechanism of their enrichment in the ANS Fe–Mn crusts and supports their independency from the major mineral phases. The present inter-elemental associations are different from the previously observed intra-crust compositional variation reported for a shallow depth (1650 m) Fe–Mn crust from the ANS (Banakar *et al* 1997), and a deep-water (5200 m) Fe–Mn crust from the Central Indian Ocean (Banakar and Hein 2000). Dissimilarity between the Pacific seamount and ANS Fe–Mn crusts also emerges from the T-REE association with the major mineral phases. The T-REE group was shown to have fractionated preferentially by the Fe-hydroxide phase in the Fe–Mn crusts from various seamounts of the Pacific (De Carlo 1991), which is not evident in the ANS Fe–Mn crusts. A weak positive correlation of T-REEs with Mn, strong negative correlation with Ti, and no correlation with Fe (table 3) render their relationship with major mineral phases complicated. The only evident weak sympathetic association of T-REEs with Mn probably suggests that to a certain extent Mn–oxide is responsible to scavenge them. However, within the T-REE a good coherence is still maintained as expected, which is also evident by the nearly flat shale normalized patterns (figure 2). We also evaluated the T-REE association with Co and Ce, which mostly exhibits weak to strong inverse relationships (see table 3 and e.g., Co vs. Lu in figure 4). Therefore, eventually the Mn–oxide appears to be the only possible principal carrier of T-REE in the ANS Fe–Mn crusts.

Except La other T-REEs exhibit insignificant variations with depth (figure 2). In that the La content in specimen occurring above 2 km depth is largely depleted by a factor of two as compared to those occurring below that depth. Interestingly the former La feature is associated with Mn contents $< 19\%$, while the latter feature with $> 21\%$ Mn content resulting in its clustering at high- and low-Mn ends (figure 4), leading to a pseudo strong co-variation ($R = 0.8$: table 3). Hence in the ANS region a hydrochemical divide might have existed at a depth of ~ 2 km. The Ce/Ce^* when plotted with depth on the ANS (figure 3), an interesting aspect of past-oxygenation in the region emerges. Except for the Fe–Mn crust at ~ 2.5 km depth that shows unusually high Ce/Ce^* (6.3) than the adjacent Fe–Mn crusts, the remaining seven samples exhibit systematically decreasing Ce/Ce^* with depth from 8.1 at 1.7 km depth to 1.6 at 3.2 km depth. An isolated behaviour of Ce/Ce^* away from a systematic trend probably indicates the exotic nature of that specimen. Alternatively, highest content of Fe and Ti, lowest content of T-REEs, and lowest Mn/Fe ratios in that specimen (table 1) possibly indicate altogether different trends in metal uptake than other samples considered here. Therefore, we ignore the metal behaviour in this sample until further investigation. Systematically decreasing Ce/Ce^* with depth clearly suggests that the oxygenation was decreasing with water depth at least up to 3.2 km in the ANS region during the past. It is noteworthy that, the southward expansion of the Arabian Sea intense OMZ around the late-Miocene time has influenced the Equatorial Indian Ocean intermediate water oxygen conditions, which also affected the ANS region (Dickens and Owen 1994). Considering these aspects we propose that, the presently intermediate depth low oxygen layer probably stood at greater water depths and was sustained for a long time in the ANS region due to increased influence of high-salinity and low-oxygen Arabian Sea OMZ waters in the low-salinity and high-oxygen EEIO. As the range of derived maximum ages (5–20 Ma) for the samples used in this study, and the uncertainty in Co-model ages are too large, it is difficult to assign a reasonable time-period at which the low oxygen layer in the ANS region was deeper than today.

Thus the compositional heterogeneity within a given Fe–Mn crust and Fe–Mn crusts from different regions and water-depths appears as a rule rather than an exception. Several previous reports have in fact clearly noted such compositional differences within the same specimen in abyssal Fe–Mn nodules and crusts of the CIO and also between samples separated by few inches on the seafloor (Glasby 1977; Moore *et al* 1981; Banakar *et al* 1989; Jauhari 1989; Banakar 1990; Banakar and Borole 1991; Frank *et al* 1999; Jauhari and Pattan 2000). Therefore the interpretation of the chemical variations in general and REE variation in particular of the seamount Fe–Mn crusts requires sample- and site-specific understanding of their growth processes.

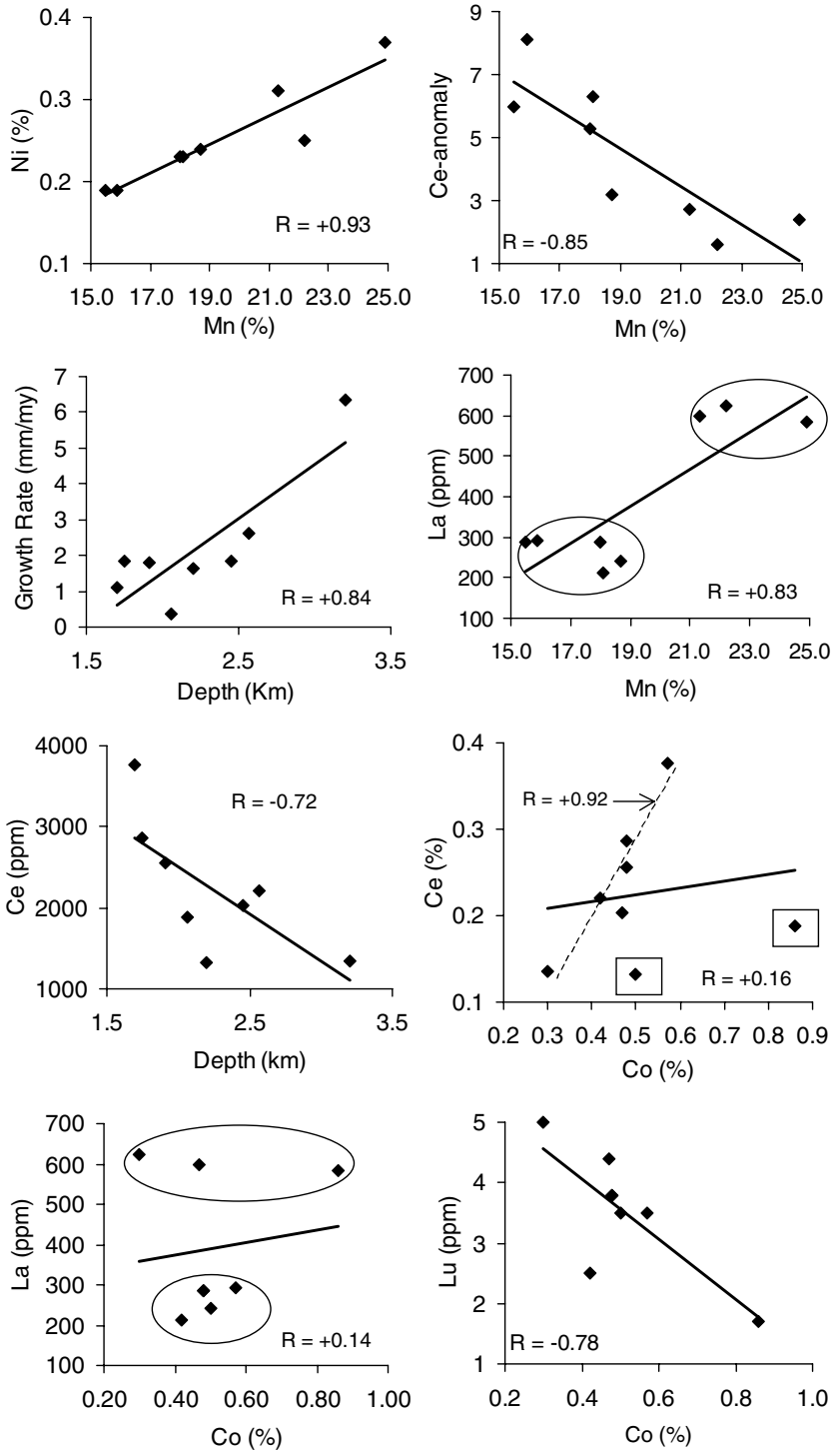

Figure 4. Scatter diagrams of few components of the crust, which describe the genetic aspects. Clustering of the data in Co versus La, and Mn versus La are shown by enclosing ovals. The two outliers in Co versus Ce diagram shown by enclosing squares significantly reduce the otherwise strong sympathetic relationship (broken best-fit) to observed negligible relationship (solid best-fit). The 'R' values are the correlation coefficients of the best fits through various data.

4. Conclusions

The Fe–Mn crusts are found to occur in the ANS region between 1700 and 3200 m water depths. The average Co-content is $\sim 0.6\%$ with a range of 0.3% to 0.8% that varies inversely with water-depth. Very low Mn/Fe ratios (< 1.5) suggest that ANS Fe–Mn crusts have formed by the hydrogenetic precipitation of hydroxide colloids.

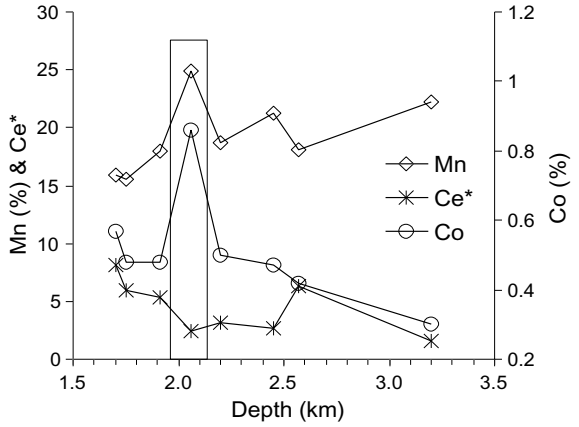

Figure 5. Variation of redox sensitive metals such as Mn, Co, and Ce-anomaly (Ce*) with water depth in the Afanasiy–Nikitin Seamount region. The vertical open bar encloses the approximate depth range at which these elements deviate sharply from the general trend.

The inter-element associations suggest that, Mn, Ni, Mo, and La, and Fe and Ti form two major groups of elements in the ANS Fe–Mn crusts, whereas, the Co and Ce appear to have precipitated together as independent oxide. The agreement in general composition and disagreement in inter-elemental relationships between the ANS region and other region Fe–Mn crusts indicate region specific fractionation of metals from the ambient seawater.

The ANS Fe–Mn crusts significantly differ from the Pacific Fe–Mn crusts in their Ce-content, whereas, most of the major and minor metals and T-REE compositions are comparable. Two- to three-fold enrichments of Ce and large Ce-anomalies in the ANS than in the Pacific Fe–Mn crusts might be the result of relatively better-oxygenated water in the hydrographic history of the ANS region. However, the modern low oxygenated intermediate depth layer in the ANS region appears to have shifted to deeper depth in the past due to southeastward expansion of the Arabian Sea intense OMZ. The layer-wise compositional variations in the ANS Fe–Mn crusts have the potential as tools for reconstructing the past changes in oceanographic conditions of the Equatorial Indian Ocean region, which forms part of our future study.

Acknowledgements

The authors wish to thank the National Institute of Oceanography for overall logistic support and the Department of Ocean Development for funding and ship-time under the Project Cobalt-crusts. The officers and crew of the R. V. A. A. Sidorenko helped in seamount sampling efforts. This manuscript is benefited by the constructive suggestions of three anonymous reviewers. The minor and REE data were obtained from the ICP-MS facility of the NGRI. RPR and ARC thank the EMR-CSIR for the award of Junior and Senior Research Fellowship respectively. This is NIO contribution no. 3922.

References

Aplin A C 1984 Rare earth element geochemistry of Central Pacific ferromanganese encrustations; *Earth Planet. Sci. Lett.* **71** 13–22.

Banakar V K 1990 Uranium–thorium isotopes and transition metal fluxes in two oriented manganese nodules from the Central Indian Basin: implications for nodule turnover; *Mar. Geol.* **95** 71–76.

Banakar V K and Borole D V 1991 Depth profiles of $^{230}Th_{excess}$, transition metals and mineralogy of ferromanganese crusts of the Central Indian basin and implications for palaeoceanographic influence on crust genesis; *Chem. Geol.* **94** 33–44.

Banakar V K and Hein J R 2000 Growth response of a deep water ferromanganese crust to evolution of the Neogene Indian Ocean; *Mar. Geol.* **162** 529–540.

Banakar V K, Pattan J N and Jauhari P 1989 Size, surface texture, chemical composition and mineralogy interrelations in ferromanganese nodules of Central Indian Ocean; *Indian J. Mar. Sci.* **18** 201–203.

Banakar V K, Pattan J N and Mudholkar A V 1997 Palaeoceanographic conditions during the formation of ferromanganese crusts from the Afanasiy–Nikitin Seamount, North Central Indian Ocean: Geochemical Evidences; *Mar. Geol.* **136** 299–315.

Bau M, Koschinsky A, Dulski P and Hein J R 1996 Comparison of the portioning behaviours of yttrium, rare earth elements, and titanium between hydrogenetic marine ferromanganese crusts and sea water; *Geochim. Cosmochim. Acta* **60** 1709–1725.

Bogorov V G and Bezrukov P L 1961 Vityaz in the Indian Ocean; *Prioda* **10** 12–35 (in Russian).

Bonatti E T, Kramer T and Rydell H 1972 Classification and genesis of submarine manganese deposits; In: Ferromanganese deposits on the Ocean Floor, (ed.) D R Horn, N S F, Washington, DC, 149–166.

Borisova A Y, Portnyagin M V, Sushchevskaya N M, Tsekhonya T I and Kononkova N N 2001 Olivine basalts of the Afanasiy–Nikitin Rise, Indian Ocean: Petrology and deuteric alteration; *Geochem. Internat.* **35** 346–358.

Burns R G and Brown B A 1972 Nucleation and mineralogical controls on the composition of manganese nodules; In: Ferromanganese deposits of the ocean floor, (ed.) D R Horn, N S F Washington DC, 51–61.

De Carlo E H 1991 Palaeoceanographic implications of rare earth element variability within a Fe–Mn crust from Central Pacific Ocean; *Mar. Geol.* **98** 449–467.

De Carlo E H and McMurtry G M 1992 Rare earth element geochemistry of ferromanganese crusts from the Hawaiian archipelago, Central Pacific; *Chem. Geol.* **95** 235–250.

Dickens G R and Owen R M 1994 Late Miocene – Early Pliocene manganese redirection in the Central Indian Ocean: Expansion of the intermediate water oxygen minimum zone; *Palaeoceanography* **9** 169–181.

Elderfield H 1988 The Oceanic chemistry of the rare earth elements; *Phil. Trans. R. Soc. London* **A 325** 105–126.

Frank M and O'Nions R K 1998 Sources of lead for Indian Ocean ferromanganese crusts: a record of Himalyan erosion? *Earth Planet Sci. Lett.* **158** 121–130.

Frank M, O'Nions R K, Hein J R and Banakar V K 1999 60 Myr records of major elements and Pb–Nd isotopes from hydrogenous ferromanganese crust: reconstruction of seawater paleochemistry; *Geochim. Cosmochim. Acta* **63** 1689–1708.

Glasby G P (ed.) 1977 Marine manganese deposits; *Elsevier Oceanogr. Ser.* **15** p. 523; Why manganese nodules remain at sediment-water interface; *New Zealand J. Sci.* **20** 187–190.

Halbach P and Puteanus D 1984 Cobalt-rich ferromanganese crusts from Central Pacific seamount regions – composition and formation; *Proc. Internat. Geol. Cong.* **6** 321–346.

Halbach P, Segl M, Puteanus D and Mangini A 1983 Co-fluxes and growth rates in ferromanganese deposits from Central Pacific seamount areas; *Nature* **304** 716–719.

Halbach P, Settler C D, Teichmann F and Wahsner M 1989 Cobalt rich platinum bearing manganese crust deposits and metal potential; *Mar. Mining* **8** 23–39.

Haskin M A and Haskin L A 1966 Rare earths in European Shale: a re-determination; *Science* **154** 507–509.

Hein J R, Schwab W C and Davis A S 1988 Cobalt and platinum rich ferromanganese crusts and associated substrate rocks from Marshall Islands; *Mar. Geol.* **78** 255–283.

Hein J R, Koschinsky A, Bau M, Manheim F T, Kang J K and Roberts L 2000 Cobalt rich ferromanganese crusts in the Pacific; In: Handbook of marine mineral deposits, (ed.) D S Cronan, C R C Press NY, *Mar. Sci. Ser.* 239–280.

Iyer S D 1991 Comparison of internal features and microchemistry of ferromanganese crusts from the Central Indian Basin; *Geo-Mar. Lett.* **11** 44–50.

Jauhari P 1989 Variability of Mn, Fe, Ni, Cu and Co in manganese nodules from the Central Indian Ocean Basin; *Mar. Geol.* **86** 237.

Jauhari P and Pattan J N 2000 Ferromanganese nodules from the Central Indian Ocean Basin; In: Handbook of marine mineral deposits, (ed.) D Cronan, C R C Press, Boca Raton, 171–195.

Koschinsky A and Halbach P 1995 Sequential leaching of marine ferromanganese precipitates: Genetic implications; *Geochim. Cosmochim. Acta* **59** 5113–5132.

Koschinsky A and Hein J R 2003 Uptake of elements from seawater by ferromanganese crusts: Solid phase association and seawater speciation; *Mar. Geol.* **198** 331–351.

Levchenko O V 1990 The geological history of the Aphanasiy–Nikitin rise, Indian Ocean; *Byul.* **65** 46–55.

Mahoney J J, White W M, Upton B G J, Neal C R and Scrutton R A 1996 Beyond EM-1: Lavas from Afanasiy–Nikitin rise and the Crozet Archipelago, Indian Ocean; *Geology* **24** 615–618.

Manheim F T and Lane-Bostwick C M 1988 Cobalt in ferromanganese crusts as a monitor of hydrothermal discharge on the Pacific seafloor; *Nature* **335** 59–62.

Moore W S, Ku T L, McDougal J D, Burns M V, Burns R, Dymond J, Lyle M W and Piper D Z 1981 Fluxes of metals to a manganese nodule: radiochemical, chemical, structural and mineralogical studies; *Earth Planet. Sci. Lett.* **52** 151–171.

Murray R W, Brink M R B, Brumsack H J, Gerlach D C and Russ III G P 1991 Rare earth elements in Japan Sea sediments and diagenetic behaviour of Ce/Ce^{*}: Results from ODP Leg 127; *Geochim. Cosmochim. Acta* **55** 2453–2466.

Parthiban G and Banakar V K 1999 Chemistry and possible resource potential of cobalt-rich ferromanganese crusts from Afanasiy–Nikitin Seamount in the Indian Ocean; *Indian Mineralogist* **33** 125–132.

Piper D Z 1974 Rare earth elements in the sedimentary cycle: a summary; *Chem. Geol.* **17** 287–297.

Rudenko M V 1994 Morphostructure of the Afanasiy–Nikitin Seamount; *Oceanology* **33** 525–530.

Sborshchikov I M, Murdmaa I O, Matveenkov V V, Kashintsev G L, Golmshtock G I and Al'mukhamedov A I 1995 Afanasiy–Nikitin Seamount within the intraplate deformation zone, Indian Ocean; *Mar. Geol.* **128** 115–126.

Segl M, Mangini A, Bonani G, Hofmann H J, Nessi M, Suter M, Wolfli W, Friedrich G, Pluger W L, Weichowski A and Beer J 1984 ^{10}Be-dating of a manganese crust from Central Pacific and implications for ocean palaeocirculation; *Nature* **309** 540–543.

Srikrishna K, Bull J M and Scrutton R A 2001 Evidence for multiphase folding of the Central Indian Ocean lithosphere; *Geology* **29** 715–718.

Verma S P, Torees-Alvarado I S and Sotelo-Rodriguez Z T 2002 SINCLAS: standard igneous norm and volcanic rock classification system; *Computers and Geoscience* **28** 711–715.

Wen X Y and De Carlo E H 1994 A comparative study of the geochemistry and internal structures of seamount ferromanganese crusts; *EOS Trans. Am. Geophys. Union* **74** 78.

Wen X, De Carlo E H and Li Y H 1997 Interelement relationship in ferromanganese crusts from the Central Pacific Ocean. Their implications for crust genesis; *Mar. Geol.* **136** 277–297.

Wyrtki K 1971 Oceanographic Atlas of the International Indian Ocean Expedition, pp. 72–156.

MS received 7 May 2004; accepted 12 August 2004